JVI Accepted Manuscript Posted Online 26 August 2015
J. Virol. doi:10.1128/JVI.01352-15
Copyright © 2015, American Society for Microbiology. All Rights Reserved.

Accepted Manuscript Posted Online
Journal of Virology
JVI
Journal of Virology

Revised Manuscript: JVI01352-15

Middle East respiratory syndrome coronavirus nsp1 inhibits host gene expression by selectively targeting nuclear-transcribed mRNAs but spares mRNAs of cytoplasmic origin

Kumari G. Lokugamage[a+], Krishna Narayanan[a+], Keisuke Nakagawa[a+], Kaori Terasaki[a], Sydney I. Ramirez[b], Chien-Te K. Tseng[a,c,d,e,f] and Shinji Makino[#,a,c,d,e,f]

Department of Microbiology and Immunology[a], Department of Pathology[b], Center for Biodefense and Emerging Infectious Diseases[c], UTMB Center for Tropical Diseases[d], Sealy Center for Vaccine Development[e], Institute for Human Infections and Immunity[f], The University of Texas Medical Branch, Galveston, Texas, USA 77555-1019

Running title: Inhibition of host gene expression by MERS-CoV nsp1

Corresponding author: Phone, 409-750-8647; E-mail, shmakino@utmb.edu.
+These authors contributed equally to this work.

Accepted Manuscript Posted Online

Journal of Virology

JVI

Abstract

The newly emerged Middle East respiratory syndrome coronavirus (MERS-CoV) and severe acute respiratory syndrome CoV (SARS-CoV) represent highly pathogenic human CoVs that share a common property to inhibit host gene expression at the post-transcriptional level. Similar to the nonstructural protein 1 (nsp1) of SARS-CoV that inhibits host gene expression at the translational level, we report that MERS-CoV nsp1 also exhibits a conserved function to negatively regulate host gene expression by inhibiting host mRNA translation and inducing the degradation of host mRNAs. Furthermore, like SARS-CoV nsp1, the mRNA degradation activity of MERS-CoV nsp1, most probably triggered by its ability to induce an endonucleolytic RNA cleavage, was separable from its translation inhibitory function. Despite these functional similarities, MERS-CoV nsp1 employed a strikingly different strategy that selectively targeted translationally-competent host mRNAs for inhibition. While SARS-CoV nsp1 is localized exclusively in the cytoplasm and binds to the 40S ribosomal subunit to gain access to translating mRNAs, MERS-CoV nsp1 was distributed in both the nucleus and cytoplasm and did not bind stably to the 40S subunit, suggesting a distinctly different mode of targeting translating mRNAs. Interestingly, consistent with this notion, MERS-CoV nsp1 selectively targeted mRNAs, which are transcribed in the nucleus and transported to the cytoplasm, for translation inhibition and mRNA degradation, but spared exogenous mRNAs introduced directly into the cytoplasm or virus-like mRNAs that originate in the cytoplasm. Collectively, these data point towards a novel viral strategy wherein the cytoplasmic origin of MERS-CoV mRNAs facilitates their escape from the inhibitory effects of MERS-CoV nsp1.

Journal of Virology

Accepted Manuscript Posted Online

Journal of Virology

JVI

Journal of Virology

48 **Importance**

49 Middle East respiratory syndrome coronavirus (MERS-CoV) is a highly
50 pathogenic human CoV that emerged in Saudi Arabia in 2012. MERS-CoV has a
51 zoonotic origin and poses a major threat to public health. However, little is known about
52 the viral factors contributing to the high virulence of MERS-CoV. Many animal viruses,
53 including CoVs, encode proteins that interfere with host gene expression, including
54 those involved in antiviral immune responses, and these viral proteins are often major
55 virulence factors. The nonstructural protein 1 (nsp1) of CoVs is one such protein that
56 inhibits host gene expression and is a major virulence factor. This study presents
57 evidence for a strategy employed by MERS-CoV nsp1 to inhibit host gene expression
58 that has not been described previously for any viral protein. The present study
59 represents a meaningful step towards a better understanding of the factors and
60 molecular mechanisms governing the virulence and pathogenesis of MERS-CoV.
61

Accepted Manuscript Posted Online

Journal of Virology

JVI

Journal of Virology

62 **Introduction**

63 Coronaviruses (CoVs) carry a single-stranded, positive-sense RNA genome of
64 approximately 30 kb and are classified into four genera: alpha, beta, gamma and delta.
65 The Middle East respiratory syndrome (MERS) CoV (MERS-CoV), a beta CoV, emerged
66 in Saudi Arabia in 2012 (1) and has spread to several other countries in the Middle East,
67 North Africa, Europe and Asia. MERS-CoV appears to have originated in bats (2), while
68 accumulating evidence has also pointed to the dromedary camels as the potential
69 animal reservoir (3, 4). MERS-CoV infection generally causes fever, cough and
70 pneumonia leading to respiratory failure and the reported case fatality rate is ~40%.
71 Some MERS patients develop acute renal failure. MERS-CoV can be transmitted from
72 person-to-person (5-7), and many cases have occurred in persons with chronic
73 underlying medical conditions or immunosuppression (8). The mechanisms governing
74 the virulence and pathogenesis of MERS-CoV are largely unknown (9).

75 Upon entry into host cells, CoV genome expression is initiated by the translation
76 of two large precursor polyproteins, pp1a and pp1ab, which are processed by viral
77 proteinases into 15-16 mature proteins; the alpha and beta CoVs encodes 16 mature
78 nonstructural proteins (nsp1 to nsp16), while the gamma and delta CoVs lack nsp1, the
79 most N-terminal cleavage product, and encode only 15 nsp's (10-12). While many of
80 these proteins play an essential role in viral RNA replication and transcription, some
81 have other biological functions as well (12). Nsp1 of alpha and beta CoVs share a
82 common biological function to inhibit host gene expression, but use different strategies
83 to exert this function (13-18). For example, nsp1 of severe acute respiratory syndrome
84 CoV (SARS-CoV), a beta CoV, uses a two-pronged strategy to inhibit host gene
85 expression (14); through its stable association with the 40S ribosomal subunit, it inhibits
86 protein synthesis by inactivating its translational function (19) and also induces host
87 mRNA degradation by triggering an endonucleolytic RNA cleavage through the possible

Accepted Manuscript Posted Online

Journal of Virology

JVI

88 recruitment of a host endonuclease (15, 20) that results in the subsequent digestion of
89 the cleavage mRNAs by the host exonuclease, Xrn1 (21). In contrast to SARS-CoV
90 nsp1, nsp1 of transmissible gastroenteritis virus (TGEV), an alpha CoV, inhibits host
91 protein synthesis without binding to the 40S subunit or inducing host mRNA degradation
92 (16). As past studies have shown that viral proteins that inhibit host gene expression are
93 major virulence factors (22, 23), nsp1 of different CoVs, with their conserved function to
94 inhibit host gene expression, most probably play a critical role in the pathogenesis of
95 CoV infections; consistent with this notion, mouse hepatitis virus nsp1 is indeed a major
96 virulence factor (17, 24). Hence, clarifying the molecular mechanisms by which the nsp1
97 of different CoVs inhibit host gene expression would contribute towards a better
98 understanding of CoV virulence and pathogenesis.
99 In this study, we report that like other CoV nsp1, MERS-CoV nsp1 also exhibits a
100 conserved function to inhibit host gene expression. A comparative analysis of SARS-
101 CoV nsp1 and MERS-CoV nsp1 revealed functional similarities but mechanistic
102 divergence among the nsp1 of these two highly pathogenic human CoVs. Our data imply
103 that MERS-CoV nsp1 inhibits host gene expression by employing a distinctly different
104 strategy that has not been described previously for any viral protein. We present
105 evidence which suggests that MERS-CoV nsp1 selectively targets the nuclear-
106 transcribed endogenous host mRNAs for inhibition whereas mRNAs that are cytoplasmic
107 in origin, including MERS-CoV mRNAs, escape the inhibitory effects of MERS-CoV
108 nsp1. We propose this property of MERS-CoV nsp1 to distinguish between cellular and
109 viral mRNAs as a novel viral escape strategy that downregulates the expression of host
110 antiviral proteins while facilitating the expression of viral proteins in MERS-CoV-infected
111 cells.
112
113 **Materials and Methods**

Journal of Virology

Accepted Manuscript Posted Online

Journal of Virology

JVI

Journal of Virology

114 **Cells and virus**

115 Vero E6 cells and BSR-T7/5 cells were grown in minimum essential medium
116 supplemented with 10% fetal bovine serum and 293 cells were maintained in Dulbecco's
117 modified Eagle's medium supplemented with 10% fetal bovine serum. The EMC/2012
118 strain of MERS-CoV (25) was grown and titrated on Vero E6 cells.

119 **Plasmid construction**

120 Human-codon optimized synthetic DNA encoding MERS-CoV nsp1 carrying a C-terminal
121 myc tag was cloned into pCAGGS-MCS, resulting in pCAGGS-MERS-CoV-nsp1.
122 Insertion of the DNA fragment encoding the codon-optimized MERS-CoV nsp1 into
123 pcDNA-MCS yielded pcDNA-MERS-nsp1. The constructs, pCAGGS-MERS-CoV-nsp1-
124 CD and pcDNA-MERS-CoV nsp1-CD, expressing a C-terminal myc-tagged MERS-CoV
125 nsp1 carrying the mutations R146A, K147A, were generated from pCAGGS-MERS-CoV-
126 nsp1 and pcDNA-MERS-nsp1, respectively, by using a recombinant PCR-based
127 method. Sequence analyses of the plasmids confirmed the expected nsp1 sequences.

128 **Generation of 293/DPP4 cells**

129 A plasmid, pCAGGS-CD26-BlasticidinR, expressing the blasticidin-resistance gene and
130 the MERS-CoV receptor, human dipeptidyl peptidase-4 (DPP4) (also known as CD26)
131 was generated by replacing the coding region of Rift Valley fever virus (RVFV) Gn/Gc
132 gene in pCAGGS-bla-G (26) with the human DPP4 gene from pcDL-SRα296 (27). 293
133 cells were transfected with pCAGGS-CD26-BlasticidinR and grown in selection medium
134 containing blasticidin (12 µg/ml) for 3 weeks. 293/DPP4 cells, stably expressing human
135 DPP4, were selected based on the resistance to blasticidin. The expression of human
136 DPP4 in 293/DPP4 cells was confirmed by Western blot analysis using anti-human
137 DPP4 antibody (R & D Systems).

138 **Plasmid transfection, reporter assays and Northern blot analysis**

Accepted Manuscript Posted Online

Journal of Virology

JVI

Journal of Virology

139 293 cells, grown in 24-well plates, were co-transfected in triplicate with various
140 combinations of plasmids (1 µg total) using the TransIT-293 reagent (Mirus). At 24 h
141 post transfection, cell lysates were prepared and subjected to Renilla luciferase (rLuc)
142 reporter activity assays (Promega). For protein expression analysis by Western blot, cell
143 extracts were prepared in sodium dodecyl sulfate-polyacrylamide gel electrophoresis
144 (SDS-PAGE) sample buffer. For RNA analysis, total RNAs were extracted, treated with
145 DNase I and subjected to Northern Blot analysis using digoxigenin-labeled antisense
146 rLuc RNA probe.

147 ***In vitro* RNA transcription, RNA transfection and RNA electroporation**

148 Capped and polyadenylated RNA transcripts, encoding chloramphenicol
149 acetyltransferase (CAT), SARS-CoV nsp1, MERS-CoV nsp1 or MERS-CoV nsp1-CD
150 proteins, were synthesized from linearized plasmids or PCR products, encoding the
151 respective genes, by using the mMESSAGE mMACHINE T7 Ultra kit (Ambion). The
152 GLA and ALA reporter mRNAs were synthesized as described previously (20). To
153 generate the MERS-CoV subgenomic mRNA 8-like RNA transcript, a PCR product
154 carrying a T7 promoter upstream of a MERS-CoV mRNA 8-like sequence, encoding the
155 viral nucleocapsid (N) gene with a C-terminal V5 epitope tag flanked by the 5' and 3'
156 untranslated regions (UTR) of MERS-CoV mRNA 8 and a poly(A) tail, was used as the
157 template. The PCR product was generated from cDNAs that were obtained from
158 intracellular RNAs extracted from MERS-CoV-infected cells. The MERS-CoV
159 subgenomic mRNA 8-like RNA transcript was synthesized from the PCR product by
160 using the mMESSAGE mMACHINE T7 in vitro transcription kit. Subconfluent 293 cells,
161 grown in 24-well plates, were transfected with *in vitro*-synthesized RNA transcripts using
162 the TransIT mRNA reagent (Mirus Madison, WI). 293 cells were electroporated with the
163 RNA transcripts using the Bio-Rad GenePulser Xcell electroporation system, according
164 to the manufacturer's instructions.

Accepted Manuscript Posted Online

Journal of Virology

JVI

Journal of Virology

165 **Metabolic radiolabeling of intracellular proteins**

166 Subconfluent 293 cells were transfected with *in vitro*-synthesized RNA transcripts and
167 incubated either in a culture medium lacking actinomycin D (ActD) or containing 4 µg/ml
168 of ActD from 1 h to 8 h post-transfection. Subsequently, the cells were starved for 30 min
169 in methionine-deficient medium and metabolically labeled with 20 µCi/ml of Tran^{35}S-label
170 (1,000 Ci/mmol; MP Biomedicals) for 1 h. The cell extracts were prepared by lysing the
171 cells in SDS-PAGE sample buffer and equivalent amounts of the extracts were analyzed
172 by SDS-PAGE. The radiolabeling of electroporated cells was performed at 24 h post-
173 electroporation with 50 µCi/ml of Tran^{35}S-label for 1 h. MERS-CoV-infected 293/DPP4
174 cells were radiolabeled with 75 µCi/ml of Tran^{35}S-label for 1 h at 18, 24 or 30 h p.i. The
175 gels were visualized by autoradiography and the band intensities in the selected regions
176 of the gel were determined by densitometric scanning of the autoradiographs.

177 **Western blot analysis**

178 Western blot analysis was performed as described previously (14). Anti-MERS-CoV-
179 nsp1 peptide antibody, generated by immunizing rabbits with the synthetic peptide
180 (RKYGRGGYHYTPFHYERD), anti-myc mouse monoclonal antibody (MAb) (Millipore)
181 and anti-V5 rabbit MAb (Abcam) were used as primary antibodies. Goat anti-mouse IgG-
182 HRP and goat anti-rabbit IgG-HRP (Santa Cruz Biotech) were used as secondary
183 antibodies.

184 **Co-sedimentation analysis**

185 Cell lysates were prepared in a lysis buffer containing 50 mM Tris-HCl (pH 7.5), 5 mM
186 $MgCl_2$, 100 mM KCl, 1% (v/v) Triton-X-100, 2 mM dithiothreitol (DTT), 100 µg/µl
187 cycloheximide and 0.5 mg/µl heparin. The lysates were applied onto a 10% to 40%
188 continuous sucrose gradient prepared in the same buffer and centrifuged at 38,000 rpm
189 in a Beckman SW41 rotor at 4°C for 3 h. After fractionation, the proteins in each fraction
190 were precipitated with trichloroacetic acid/acetone and detected by Western blot

Accepted Manuscript Posted Online

Journal of Virology

JVI

Journal of Virology

191 analysis. Total RNAs were also extracted from the fractions and the ribosomal RNAs
192 (rRNAs) were visualized by staining with ethidium bromide.

193 **Confocal microscopy analysis**

194 Cells, grown on chamber slides, were transfected with *in vitro*-transcribed RNA
195 transcripts using the TransIT-mRNA reagent. At 16 h after transfection, the cells were
196 fixed with 4% paraformaldehyde in phosphate buffered saline (PBS) for 20 min,
197 permeabilized in PBS containing 0.5% Triton X-100 for 15 min, blocked with PBS
198 containing 3% bovine serum albumin for 30 min and immunostained with anti-V5
199 antibody (Abcam). The cells were examined under a Zeiss LSM 510 UV META laser
200 scanning confocal microscope.

201 **Preparation of cytoplasmic and nuclear extracts**

202 293/DPP4 cells were infected with MERS-CoV at an m.o.i. of 3. At 18 h p.i., the cell
203 suspension was prepared and frozen at -80°C in the presence of dimethyl sulfoxide to
204 preserve the integrity of the cell membrane. The frozen cells were irradiated with 2 x10^{6}
205 rads from a Gammacell ^{60}Co source (model 109A; J. L. Shepherd and Associates, San
206 Fernando, CA) to completely inactivate MERS-CoV infectivity. After quickly thawing the
207 frozen cells, cell lysates were prepared by incubating the cells in buffer 1 (25 mM
208 HEPES, pH 7.9, 5 mM KCl, 0.5 mM $MgCl_2$, 1 mM DTT, and 0.5% NP-40 supplemented
209 with a protease inhibitor cocktail) for 15 min at 4°C. Following centrifugation at 5,000 rpm
210 for 5 min, supernatants were collected and designated as the cytoplasmic fractions. The
211 pellets were incubated in buffer 2 (25 mM HEPES, pH 7.9, 5 mM KCl, 0.5 mM $MgCl_2$, 1
212 mM DTT, and 0.25% NP-40 supplemented with a protease inhibitor cocktail) for 10 min
213 at 4°C. After centrifugation, the pellets were collected and designated as the nuclear
214 fractions (28). Essentially, the same method was used to prepare the cytoplasmic and
215 nuclear fractions from cells expressing MERS-CoV nsp1, except that the ^{60}Co irradiation
216 step was omitted.

Accepted Manuscript Posted Online

Journal of Virology

JVI

Journal of Virology

217 **Generation of RVFV-like particles (RVFV VLPs)**

218 RVFV VLPs, carrying an RNA encoding the rLuc gene (LNCR-rLuc RNA) flanked by the
219 3' and 5' noncoding regions of RVFV L RNA, were prepared as described previously
220 (29). Briefly, BSR-T7/5 cells (30), stably expressing T7 RNA polymerase, were co-
221 transfected with a plasmid expressing T7 polymerase-driven RVFV antisense LNCR-
222 rLuc RNA, along with the plasmids expressing L protein, Gn/Gc envelope proteins and N
223 protein. VLPs carrying LNCR-rLuc RNA, released into the supernatant, were collected at
224 3 days post-transfection. 293 cells were electroporated with RNA transcripts encoding
225 CAT, SARS-CoV nsp1, MERS-CoV nsp1 or MERS-CoV nsp1-CD proteins, and at 18 h
226 post-electroporation, the cells were inoculated with RVFV VLPs. As a negative control,
227 cells were inoculated with UV-irradiated VLP. Cell extracts, prepared at 6 h post-VLP
228 inoculation, were used for reporter assay and mRNA analysis.

229 **Quantitative reverse transcription-PCR (qRT-PCR)**

230 Total cellular RNAs were extracted from VLP-infected cells by using TRIzol LS reagent
231 (Invitrogen) and treated with RNase-free DNase I (Promega). cDNAs were synthesized
232 using SuperScript III reverse transcriptase (Invitrogen) and an rLuc gene-specific primer,
233 5'-TTATTGTTCATTTTTGAGAACTCGC-3', for the quantification of rLuc mRNA and
234 random primers for human 18S rRNA. RT-PCR was performed using a Bio-Rad CFX96
235 real-time PCR apparatus and SYBR Green Master mix (Bio-Rad). PCR conditions were
236 as follows: preincubation at 95°C for 30 sec and amplification with 40 cycles of 95°C for
237 15 sec and 60°C for 20 sec. The purity of the amplified PCR products was confirmed by
238 the dissociation melting curves obtained after each reaction. The primers used for rLuc
239 mRNA were 5' GCTTATCTACGTGCAAGTGATGATT-3' (forward) and 5'-
240 TAGGAAACTTCTTGGCACCTTCAAC-3' (reverse); the primers for 18S rRNA were 5'-
241 CCGGTACAGTGAAACTGCGAATG-3' (forward) and 5'-
242 GTTATCCAAGTAGGAGAGGAGCGAG-3' (reverse). The relative levels of rLuc mRNA

Accepted Manuscript Posted Online

Journal of Virology

JVI

Journal of Virology

243 normalized to 18S rRNA levels are presented in the data. All the assays were performed
244 in triplicate and the results are expressed as the mean ± standard deviation.
245
246 **Results**
247 **MERS-CoV replication inhibits host protein synthesis and promotes host mRNA**
248 **decay**
249 As a first step towards exploring the role of MERS-CoV nsp1 in the regulation of
250 host gene expression, we examined the effect of MERS-CoV replication on host protein
251 synthesis and host mRNA stability in virus-infected cells. Metabolic radiolabeling
252 experiments showed that MERS-CoV replication in 293/DPP4 cells, stably expressing
253 the MERS-CoV receptor, human DPP4 (31), induced a strong inhibition of host protein
254 synthesis, concomitant with an efficient production of virus-specific proteins, including
255 nsp1 (Fig. 1A). MERS-CoV replication also caused a substantial reduction in the levels
256 of endogenous GAPDH and β-actin mRNAs and this effect was observed both in the
257 absence or presence of actinomycin D (ActD), an inhibitor of host RNA transcription (Fig.
258 1B). Because ActD treatment prevents the synthesis of new RNAs, these data
259 demonstrated that MERS-CoV replication induced the decay of pre-existing host mRNAs
260 in infected cells. Based on our previous studies with SARS-CoV nsp1 (32), these data
261 strongly alluded to the possibility that nsp1 of MERS-CoV exerted these inhibitory effects
262 on host gene expression in virus-infected cells.
263
264 **MERS-CoV nsp1 inhibits host protein synthesis and induces endonucleolytic**
265 **cleavage and degradation of mRNAs**
266 To test the possibility that MERS-CoV nsp1 shares a common biological function
267 with SARS-CoV nsp1 to inhibit host gene expression, we transfected 293 cells with RNA
268 transcripts encoding CAT, MERS-CoV nsp1 or SARS-CoV nsp1 proteins. The

Accepted Manuscript Posted Online

Journal of Virology

JVI

Journal of Virology

269 transfected cells were incubated either in the presence or absence of ActD from 1 h
270 post-transfection and metabolically radiolabeled with Tran^{35}S-label from 8.5 to 9.5 h. Cell
271 extracts were prepared and subjected to SDS-PAGE followed by Western blot analysis.
272 The cells expressing CAT and SARS-CoV nsp1 served as negative and positive
273 controls, respectively. Like SARS-CoV nsp1, MERS-CoV nsp1 also inhibited host protein
274 synthesis both in the presence and absence of ActD (Fig. 2A). Densitometric analysis of
275 the marked areas of the gels clearly showed that the band intensities of the radiolabeled
276 host proteins in cells expressing SARS-CoV nsp1 and MERS-CoV nsp1 were lower than
277 those in cells expressing CAT (Fig. 2A). However, the extent of inhibition induced by
278 SARS-CoV nsp1 was stronger than that induced by MERS-CoV nsp1.
279 To determine whether MERS-CoV nsp1 induces the degradation of endogenous
280 host mRNAs, cells were transfected with RNA transcripts encoding CAT, MERS-CoV
281 nsp1 or SARS-CoV nsp1 proteins and incubated in the presence of ActD from 1 h post-
282 transfection. Intracellular RNAs were extracted at 1 h and 9 h post-transfection and
283 subjected to Northern blot analysis. Both MERS-CoV nsp1 and SARS-CoV-nsp1
284 expression caused a reduction in the levels of glyceraldehyde 3-phosphate
285 dehydrogenase (GAPDH) and β-actin mRNAs (Fig. 2B). Like SARS-CoV nsp1, MERS-
286 CoV nsp1 also had no effect on the ribosomal RNA levels. Because ActD treatment
287 prevents host RNA transcription, these data demonstrated that MERS-CoV nsp1
288 induced the degradation of pre-existing host mRNAs.
289 SARS-CoV nsp1 induces an endonucleolytic RNA cleavage at the 5' region of
290 capped host mRNAs as well as within the type I and II picornavirus internal ribosome
291 entry sites (IRESes), including those derived from encephalomyocarditis virus (EMCV)
292 (14, 20). Subsequently, the endonucleolytically cleaved RNAs are rapidly degraded by
293 the cellular exonuclease, Xrn I (21). To determine whether MERS-CoV nsp1 exhibited a
294 similar property to induce an endonucleolytic RNA cleavage in template mRNAs, cells

Accepted Manuscript Posted Online

Journal of Virology

JVI

295 were transfected with a plasmid encoding MERS-CoV nsp1 together with a plasmid
296 encoding a bicistronic reporter mRNA carrying the EMCV IRES between the upstream
297 Renilla luciferase (rLuc) gene and the downstream Firefly luciferase (fLuc) gene (Fig.
298 2C). As controls, expression plasmids encoding CAT or SARS-CoV nsp1 were used in
299 place of MERS-CoV nsp1. Intracellular RNAs were extracted at 24 h post-transfection
300 and subjected to Northern blot analysis. Cell extracts were also prepared at 24 h post-
301 transfection and subjected to rLuc reporter assay. MERS-CoV nsp1 expression resulted
302 in a marked reduction in the amount of the full-length Ren-EMCV-FF RNA and the extent
303 of reduction was similar to that induced by SARS-CoV nsp1 (Fig. 2C). Like SARS-CoV
304 nsp1, MERS-CoV nsp1 expression also resulted in the generation of a cleaved RNA
305 fragment derived from Ren-EMCV-FF with the same electrophoretic mobility as that
306 observed with SARS-CoV nsp1 (Fig 2C). As expected, this cleaved RNA fragment was
307 not detected in cells expressing CAT. The amount of the cleaved RNA fragment was
308 lower in MERS-CoV nsp1-expressing cells than in SARS-CoV nsp1-expressing cells.
309 Based on our previous studies that have demonstrated that the cleaved RNA fragment
310 detected in SARS-CoV nsp1-expressing cells is due to an endonucleolytic RNA
311 cleavage at the ribosome loading site of EMCV IRES (20), our data strongly implied that
312 MERS-CoV nsp1 also induced an endonucleolytic RNA cleavage at the ribosome
313 loading site of EMCV IRES.

314 A SARS-CoV nsp1 mutant carrying alanine substitutions of two charged amino
315 acid residues, R125 and K126, exposed on the surface of nsp1 (33), retained its ability
316 to inhibit translation but lacked the endonucleolytic RNA cleavage function (19). As the
317 amino acid sequence alignment of MERS-CoV nsp1 with SARS-CoV nsp1 revealed two
318 identical contiguous charged amino acids, R146 and K147, in MERS-CoV nsp1, we
319 speculated that alanine substitutions of these two charged amino acids would similarly
320 abolish the ability of MERS-CoV nsp1 to induce endonucleolytic RNA cleavage. Indeed,

Journal of Virology

Accepted Manuscript Posted Online

Journal of Virology

JVI

321 the expression of a mutated MERS-CoV nsp1, carrying R146A and K147A mutations
322 (MERS-CoV nsp1-CD) (the acronym CD stands for cleavage defective) neither induced
323 the endonucleolytic RNA cleavage in Ren-EMCV-FF RNA nor caused a reduction in the
324 abundance of the full-length Ren-EMCV-FF (Fig. 2C), demonstrating the lack of RNA
325 cleavage activity in MERS-CoV nsp1-CD and the importance of these amino acid
326 residues for the RNA cleavage function of MERS-CoV nsp1. Northern blot analysis of
327 MERS-CoV nsp1 mRNA showed that the amount of expressed RNA encoding MERS-
328 CoV nsp1 was lower than that encoding MERS-CoV nsp1-CD (Fig. 2C, second panel),
329 suggesting that MERS-CoV nsp1 targeted its own template mRNA for degradation and
330 that MERS-CoV nsp1-CD lacked the ability to degrade mRNAs. Furthermore, MERS-
331 CoV nsp1-CD expression did not cause a reduction in the amounts of GAPDH and β-
332 actin mRNAs in the presence of ActD, suggesting that MERS-CoV nsp1-CD lacked the
333 ability to induce the degradation of pre-existing host mRNAs (Fig. 2B). These data point
334 towards MERS-CoV nsp1-induced mRNA cleavage as the trigger that results in mRNA
335 degradation.

336 Like SARS-CoV nsp1, MERS-CoV nsp1 also strongly inhibited the rLuc reporter
337 activity (Fig. 2C, fourth panel). It is important to note that MERS-CoV nsp1-CD also
338 inhibited the rLuc reporter activity, albeit to a lesser extent than MERS-CoV nsp1 (Fig.
339 2C, fourth panel). Furthermore, metabolic radiolabeling experiments showed that MERS-
340 CoV nsp1-CD expression inhibited host protein synthesis but the extent of inhibition was
341 lower than that induced by MERS-CoV nsp1 (Fig. 2A). These data clearly demonstrated
342 that the RNA cleavage function of MERS-CoV nsp1 contributed to, but was not required
343 for the ability of MERS-CoV nsp1 to inhibit host protein synthesis.

344 Taken together, these data suggest that MERS-CoV nsp1 possesses two distinct
345 properties that exert an inhibitory effect on host gene expression; ability to promote the
346 accelerated turnover of host mRNAs, by inducing an endonucleolytic RNA cleavage in

Journal of Virology

Accepted Manuscript Posted Online

Journal of Virology

JVI

Journal of Virology

347 template mRNAs, and translation inhibitory function, which is separable from its RNA
348 cleavage activity.
349
350 **Subcellular localization of MERS-CoV nsp1 is different from SARS-CoV nsp1**
351 As both SARS-CoV nsp1 and MERS-CoV nsp1 exhibited similar inhibitory
352 activities on host gene expression, we sought to determine whether the two proteins
353 share a common mode of action and identify any potential mechanistic differences
354 between SARS-CoV nsp1 and MERS-CoV nsp1. To this end, we first examined the
355 subcellular localization of MERS-CoV nsp1 in transfected cells as well as in MERS-CoV-
356 infected cells. Confocal microscopy (Fig. 3A) and subcellular fractionation analyses (Fig.
357 3B) showed the distribution of MERS-CoV nsp1 and MERS-CoV nsp1-CD in both the
358 cytoplasm and nucleus of transfected cells expressing nsp1. Importantly, subcellular
359 fractionation analysis of MERS-CoV-infected cells, using an anti-MERS-CoV-nsp1
360 peptide antibody, showed a similar distribution pattern of MERS-CoV nsp1 in both the
361 cytoplasm and nucleus of MERS-CoV-infected cells (Fig. 3C). The purity of the
362 cytoplasmic and nuclear fractions was validated by Western blot analysis of the
363 subcellular fractions using anti-GAPDH and anti-histone H3 antibodies, respectively
364 (Figs. 3B, C). The distribution of MERS-CoV nsp1 in both the cytoplasm and nucleus
365 was in marked contrast to the localization of SARS-CoV nsp1 exclusively in the
366 cytoplasm (11, 15).
367
368 **MERS-CoV nsp1 and SARS-CoV nsp1 use different strategies to target**
369 **translationally-competent mRNAs for degradation**
370 The subcellular distribution of MERS-CoV nsp1 in both the cytoplasm and
371 nucleus prompted us to investigate whether MERS-CoV nsp1 also targets RNAs
372 transcribed by the nuclear RNA polymerases (Pol), Pol I and Pol III, for degradation.

Accepted Manuscript Posted Online

Journal of Virology

JVI

373 Cells were transfected with the plasmid encoding MERS-CoV nsp1 together with either
374 both Pol II-driven reporter plasmid expressing green fluorescent protein (GFP) mRNA
375 and Pol III-driven GFP plasmid or a Pol I-driven GFP reporter plasmid; the Pol I- and Pol
376 III-driven reporter plasmids encode a truncated GFP. As controls, plasmids encoding
377 CAT or SARS-CoV nsp1 were used in place of the MERS-CoV nsp1 expression
378 plasmid. Consistent with a previous report (21), SARS-CoV nsp1 expression induced the
379 degradation of only the Pol II-driven transcripts, but not the Pol I- or Pol III-driven
380 transcripts (Fig. 4A). Similarly, MERS-CoV nsp1 expression also induced the
381 degradation of only the Pol II-driven transcripts but did not affect the levels of the Pol I-
382 or Pol III-driven transcripts (Fig. 4A). A minor band migrating below the Pol III-driven
383 transcript was also observed in a published study using the same plasmid (21). The
384 source of this band is unknown. These data suggested that like SARS-CoV nsp1,
385 MERS-CoV nsp1 also targets RNAs that are translationally competent for degradation.
386 SARS-CoV nsp1 targets translating mRNAs for mRNA cleavage and translation
387 inhibition by binding to the 40S ribosomal subunit (14). To evaluate whether MERS-CoV
388 nsp1 adopted a similar strategy to gain access to translating cellular mRNAs, we
389 examined the association of MERS-CoV nsp1 with 40S subunits by sucrose gradient
390 sedimentation analysis of extracts from 293 cells expressing MERS-CoV-nsp1. Lysates
391 from cells expressing CAT or SARS-CoV nsp1 served as negative and positive controls,
392 respectively. In agreement with our previous studies (14), SARS-CoV nsp1 tightly
393 associated with the 40S subunit as demonstrated by the co-sedimentation of SARS-CoV
394 nsp1 with the 40S peak (determined by detecting 18S rRNA, a component of the 40S
395 ribosomal subunit) (Fig. 4B). In marked contrast, the sedimentation profile of MERS-CoV
396 nsp1 was very different from SARS-CoV nsp1 and mirrored the profile observed for
397 CAT. Most of the MERS-CoV nsp1 was detected near the top of the gradient and did not
398 co-sediment with the 40S subunit, suggesting that unlike SARS-CoV nsp1, MERS-CoV

Journal of Virology

Accepted Manuscript Posted Online

Journal of Virology

JVI

Journal of Virology

399 nsp1 does not associate tightly with the 40S subunit and uses a different strategy to gain
400 access to translationally-competent mRNAs (Fig. 4B).
401
402 **The translation inhibitory activity of MERS-CoV nsp1 specifically targets nuclear-**
403 **transcribed mRNAs, but spares mRNAs that enter across the cytoplasmic**
404 **membrane**
405 The lack of binding of MERS-CoV nsp1 to the 40S subunit combined with its
406 subcellular distribution in both the nucleus and cytoplasm led us to examine whether the
407 translation inhibitory activity of MERS-CoV nsp1 selectively targets mRNAs of nuclear
408 origin and spares mRNAs that enter across the cytoplasmic membrane.
409 To test the effect of MERS-CoV nsp1 on the translation of nuclear-transcribed
410 mRNAs, 293 cells were transfected with the plasmid encoding CAT, MERS-CoV nsp1,
411 MERS-CoV nsp1-CD, or SARS-CoV nsp1 together with a reporter plasmid encoding the
412 rLuc gene and assayed for luciferase reporter activity at 24 h post-transfection.
413 Intracellular RNAs were also extracted at 24 h post-transfection and subjected to
414 Northern blot analysis. As expected, SARS-CoV nsp1 strongly inhibited the reporter
415 gene activity and induced the degradation of rLuc mRNA (Fig. 5A). MERS-CoV nsp1
416 also strongly inhibited the reporter gene activity and induced the degradation of rLuc
417 mRNA (Fig 5A), which is consistent with our data in Fig. 2 that showed the inhibition of
418 host protein synthesis and induction of reporter mRNA cleavage and degradation by
419 MERS-CoV nsp1. MERS-CoV nsp1-CD did not promote the degradation of rLuc mRNA,
420 but inhibited the reporter gene activity, albeit to a slightly lesser extent than MERS-CoV
421 nsp1, further confirming that MERS-CoV nsp1-CD can inhibit translation without inducing
422 mRNA cleavage (Fig. 5A). Collectively, these data unambiguously demonstrated that
423 MERS-CoV nsp1 inhibited the translation and induced the degradation of reporter

Accepted Manuscript Posted Online

Journal of Virology

JVI

Journal of Virology

424 mRNAs as well as cellular mRNAs that are transcribed in the nucleus and transported to
425 the cytoplasm (Figs. 2, 4A and 5A).
426 To examine the effect of MERS-CoV nsp1 on the translation of exogenous
427 mRNAs introduced directly into the cytoplasm, 293 cells were electroporated with a
428 reporter mRNA, GLA, carrying the 5' UTR of rabbit β-globin mRNA and the rLuc gene
429 (20), together with RNA transcripts encoding CAT, SARS-CoV nsp1, MERS-CoV nsp1,
430 or MERS-CoV nsp1-CD; all the transcripts were capped and polyadenylated. Cell
431 extracts, prepared at 24 h post-electroporation, were subjected to luciferase reporter
432 assays and Western blot analysis. SARS-CoV nsp1 expression inhibited the reporter
433 gene activity (Fig. 5B), a result that is consistent with the ability of SARS-CoV nsp1 to
434 load onto translating mRNAs, through its association with the 40S subunit, leading to
435 translation inhibition and degradation of the electroporated GLA RNA. Strikingly, both
436 MERS-CoV-nsp1 and MERS-CoV nsp1-CD did not inhibit the luciferase reporter activity
437 (Fig. 5B). Instead, the reporter activity in cells expressing MERS-CoV nsp1 was higher
438 than in cells expressing CAT and MERS-CoV nsp1-CD (Fig. 5B). Metabolic
439 radiolabeling experiments and densitometric analysis of the marked areas of the gel
440 clearly showed that SARS-CoV nsp1, MERS-CoV nsp1 and MERS-CoV nsp1-CD
441 inhibited host protein synthesis, validating the inhibitory activity of the expressed nsp1
442 proteins towards the translation of nucleus-derived cellular mRNAs (Fig. 5B). We
443 observed slight differences in the levels of accumulation of MERS-CoV nsp1 and MERS-
444 CoV nsp1-CD, which could possibly be due to differences in the inherent stability of the
445 two proteins (Fig. 5B). We obtained similar results using a different reporter mRNA, ALA,
446 carrying the 5' UTR of β-actin mRNA and the rLuc gene (20), wherein both MERS-CoV
447 nsp1 and MERS-CoV nsp1-CD did not inhibit the reporter gene activity and an increased
448 reporter activity was observed in cells expressing MERS-CoV nsp1 (Fig. 5C).

Accepted Manuscript Posted Online

Journal of Virology

JVI

449 As MERS-CoV mRNAs are cytoplasmic in origin, we tested the effect of MERS-
450 CoV nsp1 on the translation of a MERS-CoV-like mRNA that was introduced directly into
451 the cytoplasm. 293 cells were electroporated with a MERS-CoV subgenomic mRNA 8-
452 like RNA transcript, carrying the N gene ORF with a C-terminal V5 epitope tag flanked
453 by the authentic 5' and 3' UTRs of mRNA 8 (Fig. 5D), together with RNA transcripts
454 encoding CAT, SARS-CoV nsp1, MERS-CoV nsp1, or MERS-CoV nsp1-CD. Cell
455 extracts, prepared at 24 h post-electroporation, were subjected to Western blot analysis
456 to examine the expression level of N protein. SARS-CoV nsp1 strongly inhibited the
457 expression of N protein (Fig 5D). In contrast, both MERS-CoV nsp1 and MERS-CoV
458 nsp1-CD did not inhibit the expression of N protein and the level of N protein was higher
459 in cells expressing MERS-CoV nsp1 than in cells expressing CAT and MERS-CoV nsp1-
460 CD.
461 Taken together, these data demonstrated that MERS-CoV nsp1 did not inhibit
462 the translation of exogenous reporter mRNAs and MERS-CoV-like mRNA that were
463 introduced directly into the cytoplasm. Furthermore, MERS-CoV nsp1, but not MERS-
464 CoV nsp1-CD, had a positive effect on the translation of these mRNAs, suggesting the
465 indirect role of its RNA cleavage function in this activity.
466
467 **MERS-CoV nsp1 does not inhibit the translation of virus-like mRNAs synthesized**
468 **in the cytoplasm**
469 We further extended our findings to evaluate whether MERS-CoV nsp1 also
470 spared mRNAs that are cytoplasmic in origin from its translation inhibitory activity by
471 examining the effect of MERS-CoV nsp1 on the translation of virus-like mRNAs
472 synthesized in the cytoplasm. We used VLPs derived from RVFV (family Bunyaviridae,
473 genus Phlebovirus), a cytoplasmic RNA virus, as the vehicle for the synthesis of virus-
474 like mRNAs in the cytoplasm. RVFV carries a tripartite, single-stranded, negative-sense

Journal of Virology

Accepted Manuscript Posted Online

Journal of Virology

JVI

Journal of Virology

475 RNA genome composed of L, M and S RNA segments (34). We generated RVFV VLPs,
476 carrying a single RNA segment, LNCR-rLuc RNA, encoding the rLuc reporter gene
477 flanked by the 3' and 5' noncoding regions of RVFV L RNA, from cells expressing
478 LNCR-rLuc RNA, L protein, N protein and the envelope Gn/Gc proteins, as described
479 previously (Fig. 6A) (29, 35). Inoculation of the RVFV VLPs into susceptible cells results
480 in the synthesis of LNCR-rLuc mRNAs, carrying the rLuc ORF, in the cytoplasm, due to
481 primary transcription from the incoming virion-associated LNCR-rLuc RNA mediated by
482 the virion-associated L and N proteins. However, subsequent RNA replication and
483 secondary transcription from LNCR-rLuc RNA does not occur in VLP-inoculated cells in
484 the absence of de novo synthesis of L and N proteins (35). To examine the effect of
485 MERS-CoV nsp1 on the translation and stability of cytoplasmically synthesized LNCR-
486 rLuc mRNA, 293 cells were electroporated with RNA transcripts encoding CAT, SARS-
487 CoV nsp1, MERS-CoV nsp1 or MERS-CoV nsp1-CD. At 18 h post-electroporation, cells
488 were inoculated with RVFV VLP, carrying LNCR-rLuc RNA. As a negative control, cells
489 were inoculated with UV-irradiated VLPs. Cell extracts, prepared at 6 h post-VLP
490 inoculation, were used for luciferase reporter assay, Western blot analysis, to confirm
491 the expression of proteins from the electroporated mRNAs, and the quantification of
492 LNCR-rLuc mRNA levels by qRT-PCR. As expected, very low background levels of
493 luciferase reporter activity and LNCR-rLuc mRNA were detected in cells inoculated with
494 the UV-irradiated VLP (Figs. 6B, C). The luciferase reporter activity (Fig. 6B) and LNCR-
495 rLuc mRNA levels (Fig. 6C) were substantially lower in cells expressing SARS-CoV nsp1
496 than in cells expressing CAT, demonstrating that SARS-CoV nsp1 was able to target the
497 cytoplasmically synthesized LNCR-rLuc mRNA for translation inhibition and RNA
498 degradation. In contrast, there was no statistically significant difference in the reporter
499 activity and LNCR-rLuc mRNA levels between cells expressing CAT, MERS-CoV nsp1
500 and MERS-CoV nsp1-CD, demonstrating that MERS-CoV nsp1 did not affect the

Accepted Manuscript Posted Online

Journal of Virology

JVI

Journal of Virology

501 translation and stability of cytoplasmically synthesized LNCR-rLuc mRNA (Figs. 6B, C).
502 Both SARS-CoV nsp1 and MERS-CoV nsp1 induced the degradation of endogenous
503 nucleus-derived GAPDH mRNA, confirming their biologically activity (Fig. 6C). These
504 observations further bolster the idea that MERS-CoV nsp1 specifically targets the
505 nuclear-transcribed host mRNAs for inhibition, and mRNAs, including MERS-CoV
506 mRNAs, which are cytoplasmic in origin, are spared from its inhibitory effects.
507

508 **Discussion**

509 In the present study, we first examined the effect of MERS-CoV infection on host
510 gene expression that showed similarities between MERS-CoV and another highly
511 pathogenic human CoV, SARS-CoV, in exerting an inhibitory effect on host gene
512 expression at the level of translation (15) (Fig. 1). This observation and our prior
513 knowledge of the properties of SARS-CoV nsp1 led us to investigate whether MERS-
514 CoV nsp1 shared a common function to inhibit host gene expression by targeting mRNA
515 translation and stability (32). A functional comparison between MERS-CoV nsp1 and
516 SARS-CoV nsp1 showed some common features, but also revealed intriguing
517 differences in their mechanism of action. Like SARS-CoV nsp1, MERS-CoV nsp1 also
518 exhibited two distinct properties that leads to the inhibition of host gene expression; the
519 ability to promote the degradation of host mRNAs, by inducing an endonucleolytic RNA
520 cleavage in template mRNAs, and inhibition of host mRNA translation, a function that is
521 separable from its RNA cleavage activity (Figs. 2 and 5A). Also, both MERS-CoV nsp1
522 and SARS-CoV nsp1 only targeted RNAs that are translationally competent for
523 degradation (Fig. 4A).

524 However, unlike SARS-CoV nsp1, which is localized exclusively in the cytoplasm
525 (11, 15), MERS-CoV nsp1 was distributed in both the nucleus and cytoplasm (Fig. 3).
526 Nsp1 (~9 kDa) of transmissible gastroenteritis virus (TGEV), an alpha CoV, is also

Accepted Manuscript Posted Online

Journal of Virology

JVI

Journal of Virology

527 distributed in both the nucleus and cytoplasm of transfected cells expressing nsp1 (36).
528 Although TGEV nsp1 shares a common biological function with SARS-CoV nsp1 and
529 MERS-CoV nsp1 to inhibit host gene expression, it lacks the activity to induce host
530 mRNA degradation (16). Analysis of the primary amino acid sequence of MERS-CoV
531 nsp1 did not reveal any nuclear localization signal. Although, MERS-CoV nsp1 could
532 diffuse into the nucleus because of its low molecular weight (~20 kDa), which is below
533 the size exclusion limit of the nuclear pore complex, it is also possible that its nuclear
534 accumulation could also be attributed to binding to a component of the nucleus after
535 entry by diffusion. There are examples of small viral proteins that localize to the nucleus
536 despite lacking any defined nuclear localization signal (37, 38). Importantly, the different
537 subcellular distribution profiles of MERS-CoV nsp1 and SARS-CoV nsp1 hinted at a
538 possible fundamental difference between their mechanisms of action. Indeed, while
539 SARS-CoV nsp1 associates tightly with the 40S ribosomal subunit, MERS-CoV nsp1 did
540 not co-sediment with the 40S subunit, indicating the lack of stable binding to the 40S
541 subunit (Fig. 4A). This data suggested that unlike SARS-CoV nsp1, which gains access
542 to translating mRNAs by binding to the 40S subunit (14), MERS-CoV nsp1 uses a
543 different strategy to target translationally-competent mRNAs.
544 Further evidence in support of the idea that MERS-CoV nsp1 employs a different
545 strategy to gain access to translationally-competent mRNAs was provided by the striking
546 observation that MERS-CoV nsp1 selectively inhibited the translation of nuclear-
547 transcribed mRNAs but did not inhibit the translation of mRNAs that enter across the
548 cytoplasmic membrane or are synthesized in the cytoplasm (Figs. 5 and 6). In contrast,
549 SARS-CoV nsp1 inhibited the translation of both nucleus-derived mRNAs as well as
550 mRNAs of cytoplasmic origin (Figs. 5 and 6). These data are consistent with the
551 observations that SARS-CoV nsp1 targets translating mRNAs through its association
552 with the 40S subunit, a core component of the cellular translation apparatus (14), and

Accepted Manuscript Posted Online

Journal of Virology

JVI

553 MERS-CoV nsp1 does not bind to the 40S subunit (Fig. 4A). The inability of MERS-CoV
554 nsp1 to inhibit the translation of mRNAs of cytoplasmic origin suggests that MERS-CoV
555 nsp1 does not utilize the components of the core translational machinery to gain access
556 to translating mRNAs. Additionally, it also indicates that MERS-CoV nsp1 does not affect
557 the functions of these components involved in the translation of such mRNAs.
558 MERS-CoV nsp1 displayed an intriguing property to selectively target mRNAs,
559 which are transcribed in the nucleus and transported to the cytoplasm, for translation
560 inhibition and mRNA degradation (Figs. 2, 4A and 5). Interestingly, MERS-CoV nsp1
561 inhibited host protein synthesis and induced the degradation of endogenous host
562 mRNAs even in the presence of ActD, which prevents the synthesis of new mRNAs
563 (Figs. 2A, B). These data suggested that the inhibitory activity of MERS-CoV nsp1 on
564 nucleus-derived mRNAs is not exclusively restricted to newly-synthesized mRNAs and
565 can also target pre-existing nuclear-transcribed mRNAs in the cytoplasm. The activity of
566 MERS-CoV nsp1 was directed towards different nuclear-transcribed mRNAs, including
567 endogenous host mRNAs and plasmid-driven reporter mRNAs. Eukaryotic mRNAs that
568 are transcribed in the nucleus are transported to the cytoplasm in the form of an mRNP
569 complex carrying RNA-binding proteins that regulate mRNA translation in response to
570 developmental, physiological and environmental signals (39). We speculate that MERS-
571 CoV nsp1 selectively targets nucleus-derived mRNAs, by binding to one of the mRNA-
572 binding proteins that form the host mRNP complex, and inhibits the expression of host
573 genes.
574 MERS-CoV nsp1 did not inhibit the translation of exogenous mRNAs, including
575 MERS-CoV-like mRNA, that were introduced directly into the cytoplasm (Fig. 5).
576 Furthermore, MERS-CoV nsp1 did not affect the translation and stability of a virus-like
577 mRNA synthesized in the cytoplasm (Fig. 6). These data have important implications for
578 the regulation of viral gene expression in MERS-CoV-infected cells and point towards a

Journal of Virology

Accepted Manuscript Posted Online

Journal of Virology

JVI

579 viral escape mechanism wherein MERS-CoV mRNAs, which are synthesized in the
580 cytoplasm, are spared from the inhibitory effects of MERS-CoV nsp1 on mRNA
581 translation. We hypothesize that the cytoplasmic origin of viral mRNAs facilitates their
582 escape from MERS-CoV nsp1-induced translation inhibition allowing the efficient
583 production of viral proteins. The reporter activity and the accumulation of N protein, from
584 exogenous reporter mRNAs and MERS-CoV-like mRNA, respectively, that were
585 introduced directly into the cytoplasm, was higher in cells expressing MERS-CoV nsp1
586 but not in cells expressing MERS-CoV nsp1-CD, which lacked the RNA cleavage
587 function (Fig. 5). We speculate that the degradation of endogenous host mRNAs by
588 MERS-CoV nsp1 indirectly facilitates the translation of exogenously-delivered mRNAs in
589 the cytoplasm by eliminating the translationally competent host mRNAs that compete for
590 the cellular translation machinery. However, it must be noted that this positive effect on
591 the translation of exogenously introduced mRNAs by MERS-CoV nsp1 was not
592 observed in the case of virus-like mRNAs that were synthesized in the cytoplasm (Fig.
593 6). This discrepancy could be due to differences in the experimental system and
594 template mRNAs used to evaluate the effect of MERS-CoV nsp1 on the translation of
595 mRNAs that originate in the cytoplasm. Nevertheless, this does not detract from our
596 finding that cytoplasmically synthesized virus-like mRNAs are spared from the inhibitory
597 effects of MERS-CoV nsp1. Future studies to examine the contribution of the host
598 mRNA degradation activity of MERS-CoV nsp1 on viral mRNA translation in MERS-
599 CoV-infected cells are warranted.
600

601 **Acknowledgments**

602 We thank Heinz Feldmann and Ron A. Fouchier for providing us the MERS-
603 CoV/EMC-2012 strain. We also thank Chikao Morimoto for pcDL-SRα296, Britt A.

Journal of Virology

Accepted Manuscript Posted Online

Journal of Virology

JVI

Journal of Virology

604 Glaunsinger for the pol I-, pol II- and pol III-driven GFP reporter plasmids and Adriana
605 Paulucci-Holthauzen for support with confocal microscopy analysis.
606 This work was supported by Public Health Service grants AI99107, AI101772
607 AI114657 and AI117445 from the NIH and a grant from the Institute for Human
608 Infections and Immunity at The University of Texas Medical Branch. K. Nakagawa was
609 supported by the James W. McLaughlin fellowship fund.

610

611 **References**

612 1. **Assiri A, McGeer A, Perl TM, Price CS, Al Rabeeah AA, Cummings DA,**
613 **Alabdullatif ZN, Assad M, Almulhim A, Makhdoom H, Madani H, Alhakeem**
614 **R, Al-Tawfiq JA, Cotten M, Watson SJ, Kellam P, Zumla AI, Memish ZA,**
615 **Team KM-CI.** 2013. Hospital outbreak of Middle East respiratory syndrome
616 coronavirus. N Engl J Med **369:**407-416.
617 2. **Memish ZA, Mishra N, Olival KJ, Fagbo SF, Kapoor V, Epstein JH,**
618 **Alhakeem R, Durosinloun A, Al Asmari M, Islam A, Kapoor A, Briese T,**
619 **Daszak P, Al Rabeeah AA, Lipkin WI.** 2013. Middle East respiratory syndrome
620 coronavirus in bats, saudi arabia. Emerg Infect Dis **19**.
621 3. **Briese T, Mishra N, Jain K, Zalmout IS, Jabado OJ, Karesh WB, Daszak P,**
622 **Mohammed OB, Alagaili AN, Lipkin WI.** 2014. Middle East respiratory
623 syndrome coronavirus quasispecies that include homologues of human isolates
624 revealed through whole-genome analysis and virus cultured from dromedary
625 camels in Saudi Arabia. mBio **5:**e01146-01114.
626 4. **Azhar EI, El-Kafrawy SA, Farraj SA, Hassan AM, Al-Saeed MS, Hashem AM,**
627 **Madani TA.** 2014. Evidence for camel-to-human transmission of MERS
628 coronavirus. N Engl J Med **370:**2499-2505.

Accepted Manuscript Posted Online

Journal of Virology

JVI

629 5. **Memish ZA, Zumla AI, Al-Hakeem RF, Al-Rabeeah AA, Stephens GM.** 2013.
630 Family cluster of Middle East respiratory syndrome coronavirus infections. N Engl
631 J Med **368:**2487-2494.
632 6. **Memish ZA, Zumla AI, Assiri A.** 2013. Middle East respiratory syndrome
633 coronavirus infections in health care workers. N Engl J Med **369:**884-886.
634 7. **Drosten C, Gunther S, Preiser W, van der Werf S, Brodt HR, Becker S,**
635 **Rabenau H, Panning M, Kolesnikova L, Fouchier RA, Berger A, Burguiere**
636 **AM, Cinatl J, Eickmann M, Escriou N, Grywna K, Kramme S, Manuguerra**
637 **JC, Muller S, Rickerts V, Sturmer M, Vieth S, Klenk HD, Osterhaus AD,**
638 **Schmitz H, Doerr HW.** 2003. Identification of a novel coronavirus in patients with
639 severe acute respiratory syndrome. N Engl J Med **348:**1967-1976, PMID:
640 12690091
641 8. **Guery B, Poissy J, el Mansouf L, Sejourne C, Ettahar N, Lemaire X, Vuotto**
642 **F, Goffard A, Behillil S, Enouf V, Caro V, Mailles A, Che D, Manuguerra JC,**
643 **Mathieu D, Fontanet A, van der Werf S, group ME-Cs.** 2013. Clinical features
644 and viral diagnosis of two cases of infection with Middle East Respiratory
645 Syndrome coronavirus: a report of nosocomial transmission. Lancet **381:**2265-
646 2272.
647 9. **Menachery VD, Eisfeld AJ, Schafer A, Josset L, Sims AC, Proll S, Fan S, Li**
648 **C, Neumann G, Tilton SC, Chang J, Gralinski LE, Long C, Green R, Williams**
649 **CM, Weiss J, Matzke MM, Webb-Robertson BJ, Schepmoes AA, Shukla AK,**
650 **Metz TO, Smith RD, Waters KM, Katze MG, Kawaoka Y, Baric RS.** 2014.
651 Pathogenic influenza viruses and coronaviruses utilize similar and contrasting
652 approaches to control interferon-stimulated gene responses. mBio **5:**e01174-
653 01114.

Journal of Virology

Accepted Manuscript Posted Online

Journal of Virology

JVI

654 10. **Snijder EJ, Bredenbeek PJ, Dobbe JC, Thiel V, Ziebuhr J, Poon LL, Guan Y,**
655 **Rozanov M, Spaan WJ, Gorbalenya AE.** 2003. Unique and conserved features
656 of genome and proteome of SARS-coronavirus, an early split-off from the
657 coronavirus group 2 lineage. J Mol Biol **331:**991-1004, PMID: 12927536.
658 11. **Prentice E, McAuliffe J, Lu X, Subbarao K, Denison MR.** 2004. Identification
659 and characterization of severe acute respiratory syndrome coronavirus replicase
660 proteins. J Virol **78:**9977-9986, PMCID: PMC514967.
661 12. **Newman BW, Chamberlain P, Bowden F, Joseph J.** 2014. Atlas of coronavirus
662 replicase structure. Virus Res **in press**.
663 13. **Tohya Y, Narayanan K, Kamitani W, Huang C, Lokugamage K, Makino S.**
664 2009. Suppression of host gene expression by nsp1 proteins of group 2 bat
665 coronaviruses. J Virol **83:**5282-5288.
666 14. **Kamitani W, Huang C, Narayanan K, Lokugamage KG, Makino S.** 2009. A
667 two-pronged strategy to suppress host protein synthesis by SARS coronavirus
668 Nsp1 protein. Nat Struct Mol Biol **16:**1134 -1140.
669 15. **Kamitani W, Narayanan K, Huang C, Lokugamage K, Ikegami T, Ito N, Kubo**
670 **H, Makino S.** 2006. Severe acute respiratory syndrome coronavirus nsp1 protein
671 suppresses host gene expression by promoting host mRNA degradation. Proc
672 Natl Acad Sci U S A **103:**12885-12890, PMCID: PMC1568942.
673 16. **Huang C, Lokugamage KG, Rozovics JM, Narayanan K, Semler BL, Makino**
674 **S.** 2011. Alphacoronavirus transmissible gastroenteritis virus nsp1 protein
675 suppresses protein translation in mammalian cells and in cell-free HeLa cell
676 extracts but not in rabbit reticulocyte lysate. J Virol **85:**638-643.
677 17. **Zust R, Cervantes-Barragan L, Kuri T, Blakqori G, Weber F, Ludewig B,**
678 **Thiel V.** 2007. Coronavirus non-structural protein 1 is a major pathogenicity

Journal of Virology

Accepted Manuscript Posted Online

Journal of Virology

JVI

679 factor: implications for the rational design of coronavirus vaccines. PLoS Pathog
680 **3:**e109, PMCID: PMC1941747.
681 18. **Tanaka T, Kamitani W, Dediego ML, Enjuanes L, Matsuura Y.** 2012. Severe
682 Acute Respiratory Syndrome Coronavirus nsp1 Facilitates Efficient Propagation
683 in Cells through a Specific Translational Shutoff of Host mRNA. J Virol **86:**11128-
684 11137.
685 19. **Lokugamage KG, Narayanan K, Huang C, Makino S.** 2012. Severe Acute
686 Respiratory Syndrome Coronavirus Protein nsp1 Is a Novel Eukaryotic
687 Translation Inhibitor That Represses Multiple Steps of Translation Initiation. J
688 Virol **86:**13598-13608.
689 20. **Huang C, Lokugamage KG, Rozovics JM, Narayanan K, Semler BL, Makino**
690 **S.** 2011. SARS coronavirus nsp1 protein induces template-dependent
691 endonucleolytic cleavage of mRNAs: viral mRNAs are resistant to nsp1-induced
692 RNA cleavage. PLoS Pathog **7:**e1002433.
693 21. **Gaglia MM, Covarrubias S, Wong W, Glaunsinger BA.** 2012. A common
694 strategy for host RNA degradation by divergent viruses. J Virol **86:**9527-9530.
695 22. **Smiley JR.** 2004. Herpes simplex virus virion host shutoff protein: immune
696 evasion mediated by a viral RNase? J Virol **78:**1063-1068, PMCID: PMC321390.
697 23. **Bouloy M, Janzen C, Vialat P, Khun H, Pavlovic J, Huerre M, Haller O.** 2001.
698 Genetic evidence for an interferon-antagonistic function of Rift Valley fever virus
699 nonstructural protein NSs. J Virol **75:**1371-1377.
700 24. **Zhang R, Li Y, Cowley TJ, Steinbrenner AD, Phillips JM, Yount BL, Baric**
701 **RS, Weiss SR.** 2015. The nsp1, nsp13, and M proteins contribute to the
702 hepatotropism of murine coronavirus JHM.WU. J Virol **89:**3598-3609.

Journal of Virology

Accepted Manuscript Posted Online

Journal of Virology

JVI

703 25. **Zaki AM, van Boheemen S, Bestebroer TM, Osterhaus AD, Fouchier RA.**
704 2012. Isolation of a novel coronavirus from a man with pneumonia in Saudi
705 Arabia. N Engl J Med **367:**1814-1820.
706 26. **Murakami S, Terasaki K, Ramirez SI, Morrill JC, Makino S.** 2014.
707 Development of a novel, single-cycle replicable rift valley Fever vaccine. PLoS
708 Negl Trop Dis **8:**e2746.
709 27. **Taddeo B, Esclatine A, Roizman B.** 2002. The patterns of accumulation of
710 cellular RNAs in cells infected with a wild-type and a mutant herpes simplex virus
711 1 lacking the virion host shutoff gene. Proc Natl Acad Sci U S A **99:**17031-17036.
712 28. **Rubio RM, Mora SI, Romero P, Arias CF, Lopez S.** 2013. Rotavirus prevents
713 the expression of host responses by blocking the nucleocytoplasmic transport of
714 polyadenylated mRNAs. J Virol **87:**6336-6345.
715 29. **Murakami S, Terasaki K, Narayanan K, Makino S.** 2012. Roles of the coding
716 and noncoding regions of rift valley Fever virus RNA genome segments in viral
717 RNA packaging. J Virol **86:**4034-4039.
718 30. **Buchholz UJ, Finke S, Conzelmann KK.** 1999. Generation of bovine
719 respiratory syncytial virus (BRSV) from cDNA: BRSV NS2 is not essential for
720 virus replication in tissue culture, and the human RSV leader region acts as a
721 functional BRSV genome promoter. J Virol **73:**251-259.
722 31. **Raj VS, Mou H, Smits SL, Dekkers DH, Muller MA, Dijkman R, Muth D,**
723 **Demmers JA, Zaki A, Fouchier RA, Thiel V, Drosten C, Rottier PJ,**
724 **Osterhaus AD, Bosch BJ, Haagmans BL.** 2013. Dipeptidyl peptidase 4 is a
725 functional receptor for the emerging human coronavirus-EMC. Nature **495:**251-
726 254.
727 32. **Narayanan K, Huang C, Lokugamage K, Kamitani W, Ikegami T, Tseng CT,**
728 **Makino S.** 2008. Severe acute respiratory syndrome coronavirus nsp1

Journal of Virology

Accepted Manuscript Posted Online

Journal of Virology

JVI

729 suppresses host gene expression, including that of type I interferon, in infected
730 cells. J Virol **82:**4471-4479, PMCID: PMC2293030.
731 33. **Almeida MS, Johnson MA, Herrmann T, Geralt M, Wuthrich K.** 2007. Novel
732 beta-barrel fold in the nuclear magnetic resonance structure of the replicase
733 nonstructural protein 1 from the severe acute respiratory syndrome coronavirus.
734 J Virol **81:**3151-3161, PMCID: PMC1866046.
735 34. **Terasaki K, Makino S.** 2015. Interplay between the Virus and Host in Rift Valley
736 Fever Pathogenesis. Journal of innate immunity.
737 35. **Habjan M, Penski N, Wagner V, Spiegel M, Overby AK, Kochs G, Huiskonen**
738 **JT, Weber F.** 2009. Efficient production of Rift Valley fever virus-like particles:
739 The antiviral protein MxA can inhibit primary transcription of bunyaviruses.
740 Virology **385:**400-408.
741 36. **Narayanan K, Ramirez SI, Lokugamage KG, Makino S.** 2014. Coronavirus
742 nonstructural protein 1: Common and distinct functions in the regulation of host
743 and viral gene expression. Virus Res. Nov. 26.
744 37. **Tijms MA, van der Meer Y, Snijder EJ.** 2002. Nuclear localization of non-
745 structural protein 1 and nucleocapsid protein of equine arteritis virus. J Gen Virol
746 **83:**795-800.
747 38. **Yadani FZ, Kohl A, Prehaud C, Billecocq A, Bouloy M.** 1999. The carboxy-
748 terminal acidic domain of Rift Valley Fever virus NSs protein is essential for the
749 formation of filamentous structures but not for the nuclear localization of the
750 protein. J Virol **73:**5018-5025.
751 39. **Mitchell SF, Parker R.** 2014. Principles and properties of eukaryotic mRNPs.
752 Mol Cell **54:**547-558.
753
754

Journal of Virology

Accepted Manuscript Posted Online

Journal of Virology

JVI

Journal of Virology

755 **Figure legends**

756

757 **Fig. 1. MERS-CoV replication inhibits host protein synthesis and induces host**
758 **mRNA degradation.** 293/DPP4 cells were mock-infected or infected with MERS-CoV at
759 a multiplicity of infection (m.o.i.) of 3. (A) Cells were radiolabeled with Tran^{35}S-label for 1
760 h and extracts were prepared at the indicated times post infection (p.i.). Cell lysates
761 were subjected to SDS-PAGE analysis followed by autoradiography (top left panel),
762 Western blot analysis using an anti-MERS-CoV-nsp1 peptide antibody (bottom left
763 panel) and Colloidal Coomassie blue staining (right panel). Arrowheads, MERS-CoV-
764 specific proteins. (B) Cells were incubated in the absence or presence of ActD from 1 h
765 p.i. Intracellular RNAs were extracted at 1, 18, 24 or 30 h p.i., and subjected to Northern
766 blot analysis using a GAPDH mRNA-specific probe (top panel) and β-actin mRNA-
767 specific probe (middle panel). The amounts of 28S and 18S rRNAs in each sample were
768 detected by ethidium bromide staining (bottom panel).

769

770 **Fig. 2. MERS-CoV nsp1 inhibits host protein synthesis and induces**
771 **endonucleolytic cleavage and degradation of mRNAs.** (A) 293 cells were
772 transfected with RNA transcripts encoding CAT, SARS-CoV nsp1, MERS-CoV nsp1 or
773 MERS-CoV nsp1-CD proteins, carrying a C-terminal myc epitope tag, and incubated in
774 the absence or presence of ActD from 1 h post-transfection. Cells were radiolabeled with
775 Tran^{35}S-label from 8.5 to 9.5 h post-transfection and lysates were resolved on 12%
776 SDS-PAGE followed by autoradiography (top panels), Colloidal Coomassie blue staining
777 (middle panels) and Western blot analysis using anti-myc antibody (bottom panels).
778 Densitometric analysis of the autoradiographs was used to determine the levels of host
779 protein synthesis, and the numbers below the lanes in the top panels represent
780 percentage band intensity relative to CAT RNA-transfected cells (% of CAT). The box

Accepted Manuscript Posted Online

Journal of Virology

JVI

Journal of Virology

781 represents the region of the gel used for densitometric analysis. Representative data
782 from three independent experiments are shown. (B) 293 cells were transfected with RNA
783 transcripts encoding CAT, SARS-CoV nsp1, MERS-CoV nsp1 or MERS-CoV nsp1-CD
784 and incubated in the presence of ActD from 1 h post-transfection. At 1 h and 9 h post
785 transfection, intracellular RNAs were extracted and subjected to Northern blot analysis
786 using a GAPDH mRNA-specific probe (top panels) and β-actin mRNA-specific probe
787 (middle panels). The bottom panel represents the amounts of 28S and 18S rRNAs in
788 each sample. (C) 293 cells were co-transfected with a plasmid encoding Ren-EMCV-FF
789 and the plasmid expressing CAT, SARS-CoV nsp1, MERS-CoV nsp1 or MERS-CoV
790 nsp1-CD; the nsp1-expression plasmids encoded proteins carrying the C-terminal myc
791 tag. At 24 h post-transfection, intracellular RNAs were extracted and subjected to
792 Northern blot analysis using an RNA probe that binds to the rLuc gene (top panel) and
793 MERS-CoV nsp1 gene (second panel), respectively. The 28S and 18S rRNAs were
794 detected by ethidium bromide staining (third panel). Cell extracts, prepared at 24 h post-
795 electroporation, were used for a reporter assay (fourth panel) and Western blot analysis,
796 using an anti-myc antibody (bottom panel). Arrowhead, full-length Ren-EMCV-FF; arrow,
797 cleaved RNA fragment. A schematic diagram of Ren-EMCV-FF RNA is shown on top.
798
799 **Fig. 3. Subcellular distribution of MERS-CoV nsp1 in both the nucleus and**
800 **cytoplasm.** (A) Vero E6 cells were mock-transfected (a) or transfected with RNA
801 transcripts encoding C-terminal V5-tagged MERS-CoV nsp1 (b) or MERS-CoV nsp1-CD
802 (c). At 16 h after transfection, the cells were fixed, permeabilized and subjected to
803 immunofluorescence analysis using an anti-V5 antibody (Anti-V5). The nuclei were
804 counterstained with 4′, 6-diamidino-2-phenylindole (DAPI) and the images were
805 examined using a Zeiss LSM 510 UV META laser scanning confocal microscope.
806 Merged images are shown in the rightmost panels. (B) 293 cells were mock-transfected

Accepted Manuscript Posted Online

Journal of Virology

JVI

807 (Mock) or transfected with a plasmid encoding the C-terminal myc-tagged MERS-CoV
808 nsp1 (MERS-CoV nsp1) or MERS-CoV nsp1-CD (MERS-CoV nsp1-CD). At 18 h post-
809 transfection, cell lysates were fractionated into cytoplasmic and nuclear fractions.
810 Subsequently, the fractions were subjected to Western blot analysis using anti-myc (top
811 panels), anti-histone H3 (middle panels) and anti-GAPDH antibodies (bottom panels).
812 The asterisks in the top panels represent possible proteolytic cleavage products of
813 MERS-CoV nsp1 and MERS-CoV nsp1-CD, probably generated during sample
814 preparation. (C) 293/DPP4 cells were mock-infected (Mock) or infected with MERS-CoV
815 at an m.o.i. of 3 (MERS-CoV). At 18 h p.i., the cell suspension was irradiated with ^{60}Co
816 to inactivate MERS-CoV and cell extracts were separated into cytoplasmic and nuclear
817 fractions. Each fraction was subjected to Western blot analysis using anti-MERS-CoV-
818 nsp1 peptide antibody (top panels), anti-histone H3 antibody (middle panels) or anti-
819 GAPDH antibody (bottom panels). The asterisks (mock-infected cell extracts, top panels)
820 represent a host protein with a slower migration than nsp1 in the gel that is recognized
821 nonspecifically by the anti-MERS-CoV-nsp1 peptide antibody.
822
823 **Fig. 4. MERS-CoV nsp1 targets translationally-competent Pol II-transcribed**
824 **mRNAs for degradation but does not co-sediment with 40S ribosomal subunits.**
825 (A) 293 cells were transfected with a plasmid encoding CAT, SARS-CoV nsp1 or MERS-
826 CoV nsp1 together with Pol II- and Pol III-driven reporter plasmids encoding GFP RNA
827 or a Pol I-driven GFP reporter plasmid. At 24 h post-transfection, RNAs were extracted,
828 treated with DNase I and visualized by Northern blot using a GFP-specific probe. The
829 28S and 18S rRNAs were detected by ethidium bromide staining (bottom panels). (B)
830 293 cells were transfected with RNA transcripts encoding C-terminal myc-tagged CAT
831 (panels a and b), SARS-CoV nsp1 (panels c and d) or MERS-CoV-nsp1 (panels e and
832 f). Cell extracts, prepared at 8 h post-transfection, were subjected to sucrose gradient

Journal of Virology

Accepted Manuscript Posted Online

Journal of Virology

JVI

Journal of Virology

833 centrifugation analysis. The gradient fractions were analyzed by Western blot using anti-
834 myc antibody to detect the expressed proteins (panels, a, c and e) and ethidium bromide
835 staining to detect rRNAs (panels b, d, and f).
836
837 **Fig. 5. MERS-CoV nsp1 does not inhibit the translation of mRNAs introduced**
838 **directly into the cytoplasm** (A) 293 cells were transfected with the reporter plasmid
839 pRL-SV40 (15) encoding the rLuc gene together with the expression plasmids encoding
840 CAT, SARS-CoV nsp1, MERS-CoV nsp1 or MERS-CoV nsp1-CD; the nsp1 proteins had
841 a C-terminal myc tag. Cell extracts, prepared at 24 h post-transfection, were used for a
842 reporter assay (top panel) and Western blot analysis, using anti-myc antibody (second
843 panel). Intracellular RNAs were also extracted at 24 h post-transfection, and subjected to
844 Northern blot analysis using the RNA probe that binds to the rLuc gene (third panel). The
845 28S and 18S rRNAs were detected by ethidium bromide staining (bottom panel).
846 Representative data from three independent experiments is shown. (B) 293 cells were
847 co-electroporated with GLA reporter mRNA and RNA transcripts encoding C-terminal
848 myc-tagged CAT, SARS-CoV nsp1, MERS-CoV nsp1 or MERS-CoV nsp1-CD. Cell
849 extracts, prepared at 24 h post-electroporation, were used for the reporter assay (left top
850 panel) and Western blot analysis, using anti-myc antibody (left bottom panel).
851 Representative data from three independent experiments is shown. Asterisks indicate
852 statistically significant differences between samples ($p< 0.01$); ns, not significant ($p>$
853 0.01). Cells that were electroporated with the RNA transcripts were also radiolabeled
854 with Tran^{35}S-label for 1 h at 24 h post-electroporation and lysates were resolved on
855 SDS-PAGE followed by autoradiography (right top panel), Colloidal Coomassie blue
856 staining (right middle panel) and Western blot analysis using anti-myc antibody (right
857 bottom panel). Densitometric analysis of the autoradiographs was used to determine the
858 levels of host protein synthesis, and the numbers below the lanes in the right top panel

Accepted Manuscript Posted Online

Journal of Virology

JVI

Journal of Virology

859 represent percentage band intensity relative to CAT RNA-transfected cells (% of CAT).
860 The box represents the region of the gel used for densitometric analysis. Representative
861 data from three independent experiments is shown. (C) RNA co-electroporation and
862 reporter assay were performed as described in (B), except that ALA reporter mRNA was
863 used in place of the GLA mRNA. Representative data from three independent
864 experiments is shown. Asterisks indicate statistically significant differences between
865 samples ($p < 0.01$); ns, not significant ($p > 0.01$). (D) RNA co-electroporation was
866 performed as described in (B), except that a MERS-CoV subgenomic mRNA 8-like RNA
867 transcript, expressing a C-terminal V5-tagged MERS-CoV N protein, was used in place
868 of the GLA mRNA. Cell extracts, prepared at 24 h post-electroporation, were subjected
869 to Western blot analysis using anti-V5 antibody (top panel), anti-myc antibody (middle)
870 and anti-actin antibody (bottom). The asterisk in the top panel represents a host protein
871 that is recognized nonspecifically by the anti-V5 antibody. A schematic diagram of the
872 MERS-CoV subgenomic mRNA 8-like RNA transcript is shown on top.
873
874 **Fig. 6. MERS-CoV nsp1 does not inhibit the translation of virus-like mRNAs**
875 **synthesized in the cytoplasm** (A) Schematic diagram of the experimental approach.
876 BSR-T7/5 cells, stably expressing T7 RNA polymerase, were co-transfected with a
877 plasmid expressing T7 polymerase-driven RVFV antisense LNCR-rLuc RNA, along with
878 the plasmids expressing L protein, Gn/Gc envelope proteins and N protein. VLPs
879 carrying LNCR-rLuc RNA, released into the supernatant, were collected at 3 days post-
880 transfection. 293 cells were electroporated with RNA transcripts encoding CAT, SARS-
881 CoV nsp1, MERS-CoV nsp1 or MERS-CoV nsp1-CD proteins and at 18 h post-
882 electroporation, the cells were inoculated with RVFV VLPs. As a negative control, cells
883 were inoculated with UV-irradiated VLP. Cell extracts, prepared at 6 h post-VLP
884 inoculation, were used for reporter assay, protein expression and mRNA analyses. (B)

Accepted Manuscript Posted Online

Journal of Virology

JVI

885 Top panel shows the luciferase reporter activities at 6 h post-VLP inoculation. Bottom
886 panel represents the Western blot analysis using anti-myc antibody. (C) Intracellular
887 RNAs were extracted at 6 h post-VLP inoculation and subjected to qRT-PCR to
888 determine the levels of LNCR-rLuc mRNA and 18S rRNA. The plot shows the relative
889 levels of LNCR-rLuc mRNA normalized to 18S rRNA levels. Bottom panel shows the
890 Northern blot analysis of GAPDH mRNA. Error bars in the plot represent standard
891 deviation of three independent experiments. Asterisks indicate statistically significant
892 differences between samples ($p < 0.01$); ns, not significant ($p > 0.01$).

Journal of Virology

Accepted Manuscript Posted Online

Journal of Virology

JVI

Journal of Virology

Fig.1

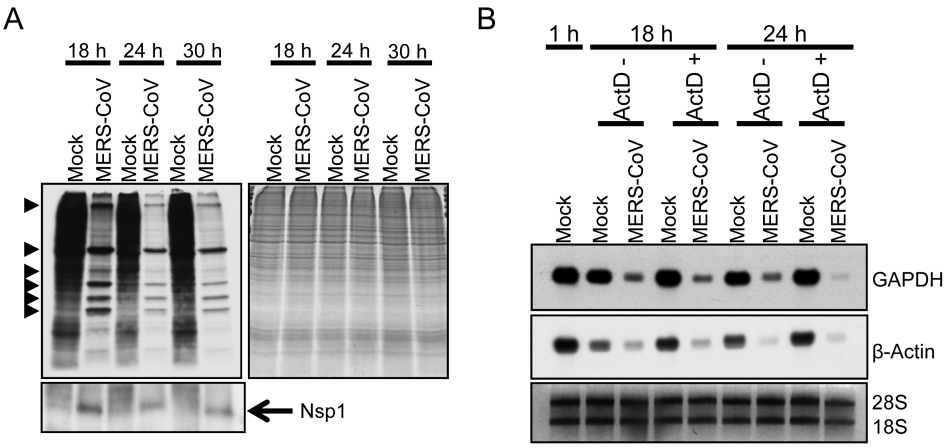

Accepted Manuscript Posted Online
Journal of Virology
JVI
Journal of Virology

Fig.2

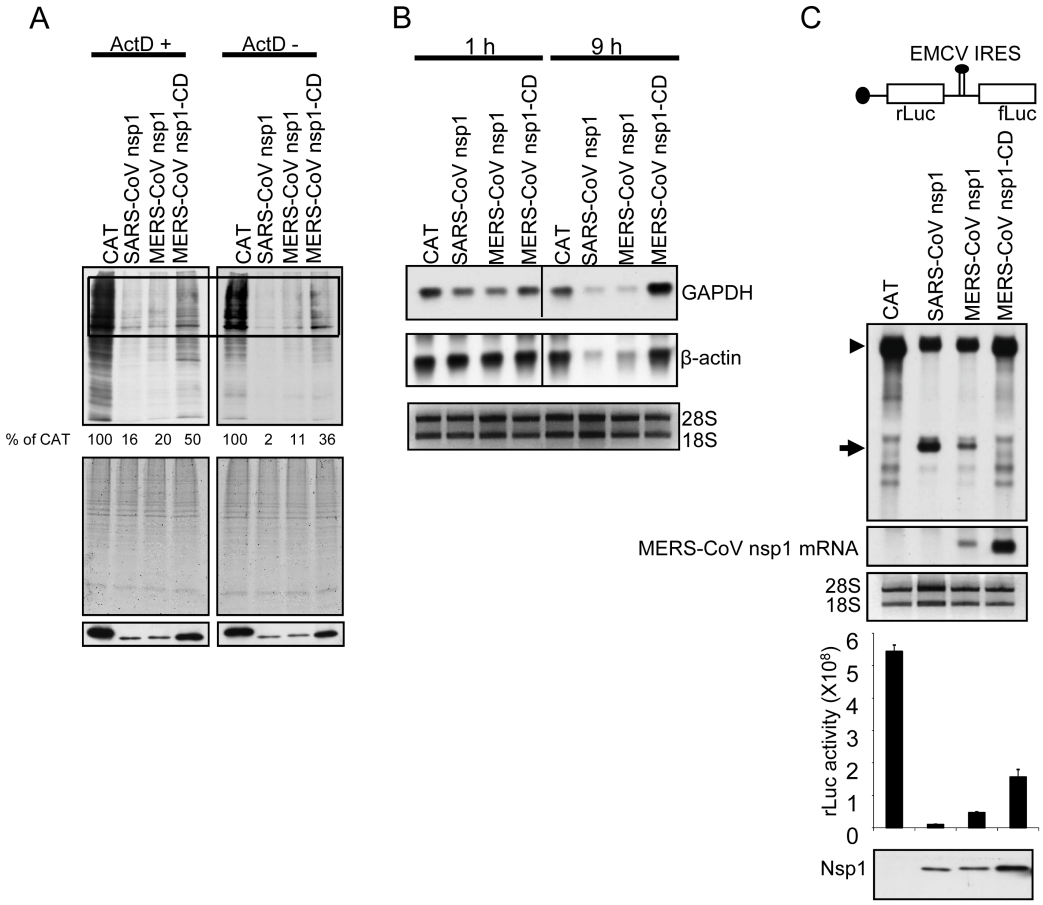

Accepted Manuscript Posted Online

Journal of Virology

JVI

Journal of Virology

Fig.3

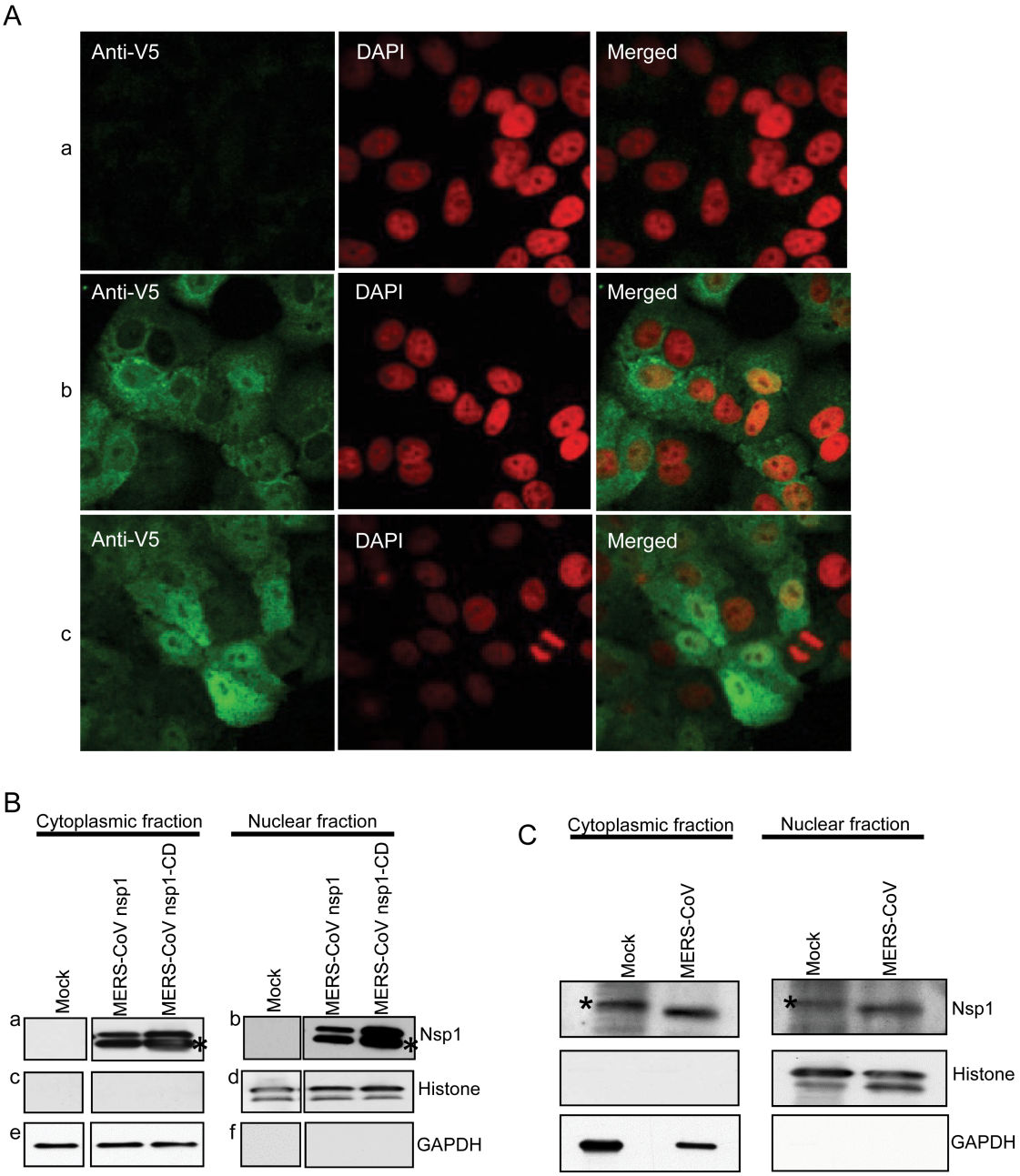

Accepted Manuscript Posted Online

Journal of Virology

JVI

Journal of Virology

Fig.4

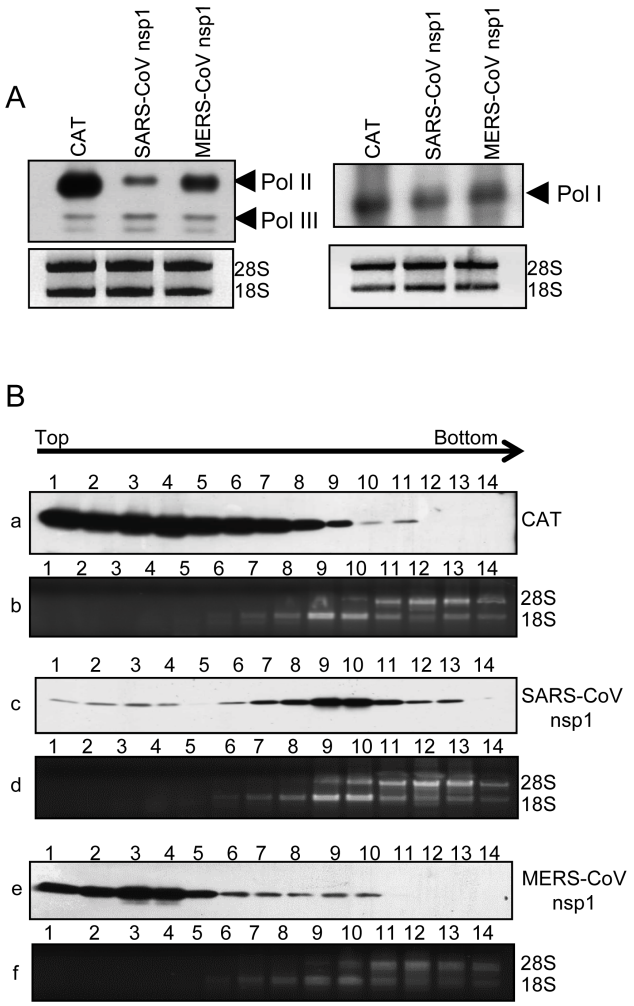

Accepted Manuscript Posted Online
Journal of Virology
JVI
Journal of Virology

Fig.5

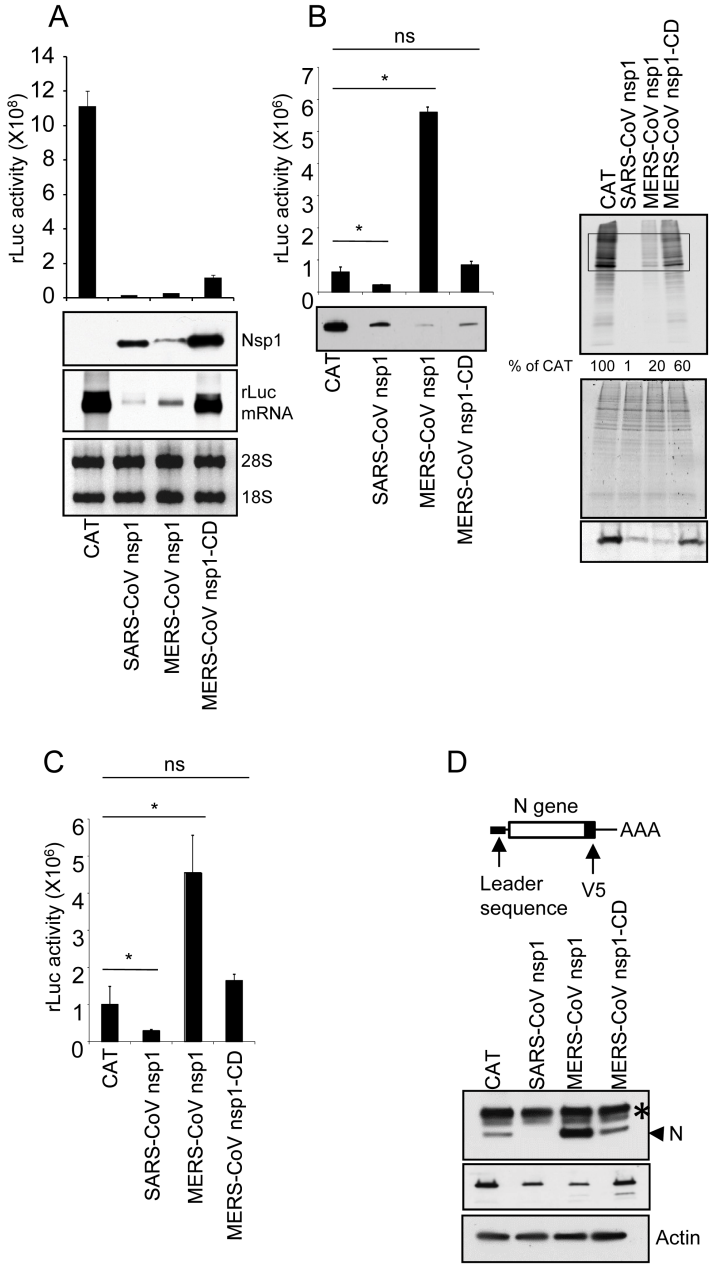

Accepted Manuscript Posted Online

Journal of Virology

JVI

Journal of Virology

Fig.6